Efficient preparation of 5,10,15,20-tetrakis(4-bromophenyl)porphyrin. Microwave assisted v/s conventional synthetic method, X-ray and hirshfeld surface structural analysis

Edison Matamala-Cea, Fabian Valenzuela-Godoy, Déborah González, Rodrigo Arancibia, Vincent Dorcet, Jean-René Hamon, Nestor Novoa

▶ **To cite this version:**

Edison Matamala-Cea, Fabian Valenzuela-Godoy, Déborah González, Rodrigo Arancibia, Vincent Dorcet, et al.. Efficient preparation of 5,10,15,20-tetrakis(4-bromophenyl)porphyrin. Microwave assisted v/s conventional synthetic method, X-ray and hirshfeld surface structural analysis. Journal of Molecular Structure, 2020, 1201, pp.127139. 10.1016/j.molstruc.2019.127139 . hal-02367901

HAL Id: hal-02367901

https://univ-rennes.hal.science/hal-02367901v1

Submitted on 17 Feb 2020

HAL is a multi-disciplinary open access archive for the deposit and dissemination of scientific research documents, whether they are published or not. The documents may come from teaching and research institutions in France or abroad, or from public or private research centers.

L'archive ouverte pluridisciplinaire **HAL**, est destinée au dépôt et à la diffusion de documents scientifiques de niveau recherche, publiés ou non, émanant des établissements d'enseignement et de recherche français ou étrangers, des laboratoires publics ou privés.

Efficient preparation of 5,10,15,20-*tetrakis*(4-bromophenyl)porphyrin. Microwave assisted *v/s* conventional synthetic method, X-ray and Hirshfeld surface structural analysis

Edison Matamala-Cea[a], Fabián Valenzuela-Godoy[a], Déborah González[a], Rodrigo Arancibia[a], Vincent Dorcet[b], Jean-René Hamon[b,*], Néstor Novoa[a,*]

a *Laboratorio de Química Inorgánica y Organometálica, Departamento de Química Analítica e Inorgánica, Facultad de Ciencias Químicas, Universidad de Concepción, Edmundo Larenas 129, Casilla 160-C, Concepción, Chile.*

b *Univ Rennes, CNRS, ISCR (Institut des Sciences Chimiques de Rennes) – UMR 6226, F-35000 Rennes, France.*

* Corresponding authors.
E-mail address: jean-rene.hamon@univ-rennes1.fr (J.-R. Hamon)
E-mail address: nenovoa@udec.cl (N. Novoa)

Accepted manuscript

Abstract:

The symmetrical *meso*-tetrasubstituted porphyrin 5,10,15,20-*tetrakis*(4-bromophenyl)Porphyrin (**1)** has been synthesized in quite high yields, ranging from 55 to 78%, by conventional and microwave assisted techniques, and isolated as a microcrystalline compound. The products obtained in each case have been characterized by ^{1}H-NMR, Mass spectrometry, elemental analysis and Thin layer chromatography. The X-ray crystal structure of **1** is reported for the first time, and reveals a planar disposition of the center of the macrocycles with almost orthogonal 4-bromophenyl rings in the four *meso*-positions in the solid state. Hirshfeld surface (HS) analysis along with 2D fingerprint plots were employed to consider the intermolecular forces, including hydrogen bonds and π–π stacking interactions, and their quantification in the crystal lattice.

Keywords

Meso-tetraporphyrins

Microwave assisted synthesis

Single crystal X-ray Diffraction

Hirshfeld Surface Analysis

Accepted manuscript

1. Introduction

Porphyrin, a square planar 18-π aromatic macrocycle consisting of four pyrroles and four methine carbons, is arguably the most significant pigment to be found in nature [1,2]. Owing to the well-known advantageous properties such a structural robustness, attractive absorption and emission properties, strong aromaticity and rich metal coordination chemistry, porphyrins have been broadly used in a wide range of research disciplines [1–9]. The recognition of porphyrins as molecular system susceptible to conjugative perturbations at the periphery of the coordination center, allows rationalizing electronic fine-tuning modifications in the molecular unit that affords systems displaying drastically altered optical and electronic properties [1–9]. In this context, the extensive number of functionalizable positions of the macrocycle (12) offers a large panel of possible molecular designs for porphyrins [1,5] as ligands and metalloligands (see Chart 1). Particularly, the *meso*-substituted porphyrins are relatively easy to prepare showing high versatility that allows many possible designs for porphyrin-based ligands and derived coordination compounds. However, the conventional methods to prepare this kind of substituted macrocycles give low yield and use large volume of organic solvent and prolonged reaction times, often followed by tedious chromatographic purification [10-13]. To circumvent these drawbacks, solventless syntheses of *meso*-tetrasubstituted porphyrins have been reported, involving either a two-step mechanochemical process (condensation followed by oxidation) [14], or mixing the two reagents in the gas phase at very high temperature (>200°C) [15], or microwave-mediated synthesis on solid support [16,17]. Nevertheless, those above methods still suffer from low yields (1-25%). By contrast, variously substituted 5,10,15,20-tetraarylporphyrins were shown to be readily accessible in yields up to 43% via microwave-assisted cyclocondensation of different aryl aldehydes with pyrrole, using a minimum amount of propionic acid [18]. Thus, microwave irradiation, also useful in metalloporphyrin synthesis [17,19], appears as a straightforward one-pot practical methodology minimizing reaction time, amount of solvent, and work-up problems.

Bromo substituted tetrapyrrolic derivatives, such as the symmetrical 5,10,15,20-*tetrakis*(4-bromophenyl)porphyrin (**1**) prepared for the first time by J.B. Kim and co-workers in the early 70's in 12% isolated yield [20], have been broadly reported as very important building blocks for molecular material applications by efficient bottom-up

Accepted manuscript

synthesis through organometallic methodologies, *e.g.* Heck [21,22], Sonogashira, Negishi, Stille, Suzuki, Click, and others cross coupling reactions [22]. In this regard, this piece of work reports on a comparison between a conventional heating two step synthesis *v/s* a microwave assisted (one-pot) improved high yield (> 55%) synthesis of **1**, its full analytical and spectral characterization, and its crystallographic and Hirshfeld Surface study in the solid state.

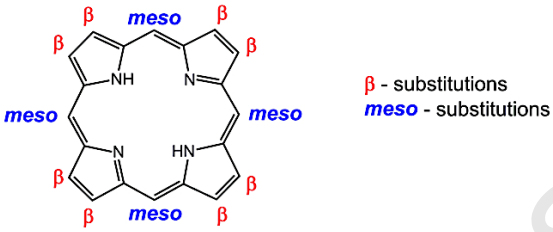

Chart 1. Four *meso*- and eight β-position available to modify the porphyrinic macrocycle.

2. Experimental Section

2.1. General considerations

All reactions were performed under dinitrogen atmosphere using standard Schlenk techniques. The solvents were dried and distilled according to standard procedures [23]. 1*H*-Pyrrole, propionic acid, 4-bromobenzaldehyde, $BF_3{\cdot}OEt_2$ and *p*-chloranil were purchased from commercial sources and used without further purification. Microwave reactions were carried out in a Microwave Synthesizer Biotage® Initiator+. ^1H NMR spectra were recorded on a Bruker Advance 400 Digital Instrument. All NMR spectra are reported in parts per million (ppm, δ) relative to tetramethylsilane (Me_4Si), with the residual solvent proton resonances used as internal standards. Elemental analyses were measured on a Perkin Elmer CHN Analyzer 2400. Mass spectra were obtained at the Laboratorio de Servicios Analíticos, Pontificia Universidad Católica de Valparaíso, Valparaíso, Chile.

Accepted manuscript

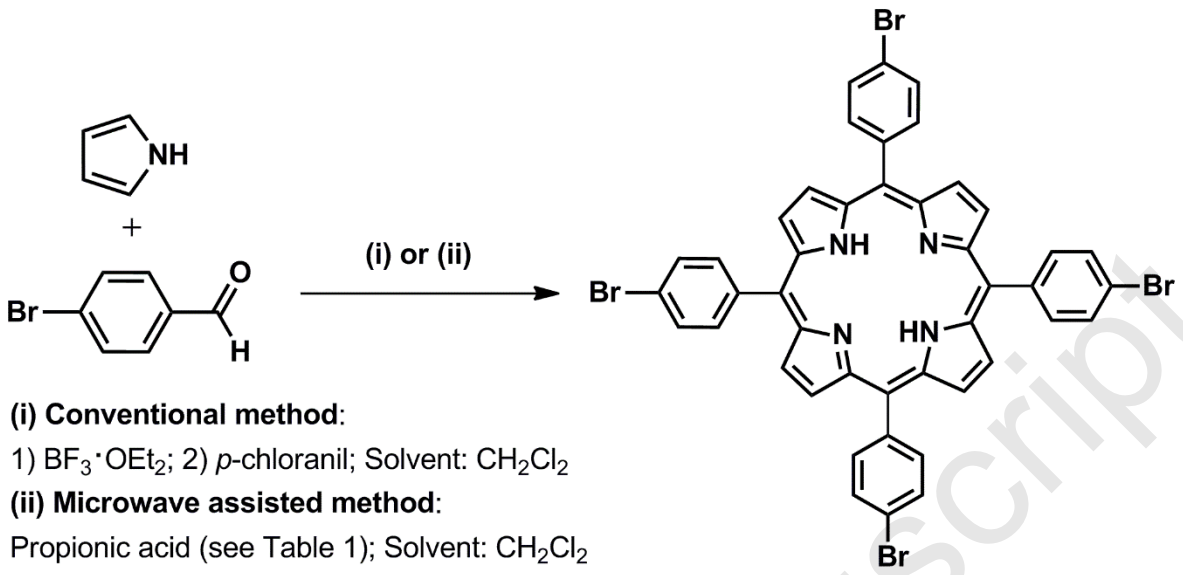

Scheme 1. Synthesis of the 5,10,15,20-*tetrakis*(4-bromophenyl)porphyrin **1** *via* conventional and microwave-mediated methods.

*2.2. Preparation of 5,10,15,20-tetrakis(4-bromophenyl)porphyrin (**1**):*

2.2.1. Synthesis via modified conventional method

The reaction was carried out following an similar method to that reported by Drouet *et al* for the synthesis of 5,10,15,20-tetrakis(4-trimethylsilylethynylphenyl)porphyrin [24]. A two necked round bottom flask was loaded with a magnetic stir bar, 0.7 mL (10 mmol) of freshly distilled 1*H*-Pyrrole, 1.85 g (10 mmol) of 4-bromobenzaldehyde and 100 mL of CH_2Cl_2. Then, 0.4 mL (3.0 mmol) of $BF_3{\cdot}OEt_2$ was added and the resulting mixture was stirred vigorously at room temperature in the dark for 3 h. After that time, 1.84 g (7.50 mmol) of *p*-chloranil was added to the reaction mixture that was refluxed for 1h. The resulting black mixture was cooled at room temperature, filtered over a silica gel:celite® (1:1 ratio) mixture, and rinsed several times with $CHCl_3$. The collected fractions were concentrated under vacuum, and the resulting black solid material was absorbed on silica gel (70 mesh, 256) packed column, and eluted with CH_2Cl_2: hexane (7:3, *v*:*v*) mixture. The dark-purple band was collected and the solvent was completely removed under reduced pressure, giving a microcrystalline purple compound that was further dried under vacuum

Accepted manuscript

for 3 h. Yield: 512 mg (0.55 mmol, 55%). ^{1}H-NMR ($CDCl_3$, 21ºC): δH -2.85 (s, 2H, NH); 7.83 (d, ^{3}J=8.2 Hz, 8H, H 3,5-phenyl); 7.99 (d, ^{3}J=8.2 Hz, 8H, H 2,6-phenyl); 8.77 (s, 8H, H of β-pyrrole). MS: *m/z* calc. for $C_{44}H_{26}{}^{79}Br_4N_4$: 929.89; found: 929.80 [M^+]. Anal. Calc. for $C_{44}H_{26}Br_4N_4$: C, 56.81; H, 2.82; N, 6.02. Found: C, 56.70; H, 2.65; N, 6.09. Recrystallization from vapor diffusion of diethyl ether into $CHCl_3$ solution of the compound for 7 days at room temperature (1:5, *v*:*v*), afforded blue microcrystals of **1** suitable for single-crystal X-ray diffraction.

2.2.2. Synthesis via Microwave assisted method

A vial was charged with 0.7 mL (10 mmol) of freshly distilled 1*H*-Pyrrole, 1.85 g (10 mmol) of 4-bromobenzaldehyde, 10 mL of CH_2Cl_2, and the appropriate volume of propionic acid of each entry depicted in table 1. The vial was capped with Teflon, deposited in a Microwave reactor for 2 minutes at 300 W, cooled and gently stirred at room temperature for 5 min, and put back in the Microwave reactor. This procedure was repeated ten times for each trial, affording a black oil in each case. The crude products were purified using the same chromatographic method described in the previous section. The obtained yields are listed in table 1, and the isolated purple solids were authenticated by ^{1}H NMR, Mass spectrometry and Thin layer chromatography on silica gel (R_f = 0.95, $CHCl_3$:petroleum ether 8:2 mixture (*v*:*v*)).

Table 1 Reaction conditions for microwave assisted preparation of *5,10,15,20-tetrakis(4-bromophenyl)porphyrin* (**1**).

Entry	Time of reaction (minutes)	Propionic acid volume (mL)	Yield (%)
1	20	0.5	40
2	20	1.0	78
3	20	1.5	48
4	20	2.0	35
5	20	2.5	20
6	20	3.0	8

Accepted manuscript

2.3. X-ray structure determination

A well-shaped crystal of compound **1** was coated in Paratone-N oil, mounted on a nylon loop and transferred to the cold gas stream of the cooling device. Intensity data were collected at 150(2) K on a D8 VENTURE Bruker-AXS diffractometer equipped with a multilayer monochromated Mo-Kα radiation (λ = 0.71073 Å) and a CMOS Photon100 detector. The structure was solved by dual-space algorithm using the SHELXT program [25], and then refined with full-matrix least-square method based on F^2 (SHELXL-2014) [26]. The contribution of the disordered diethyl ether molecules (four per unit cell) to the calculated structure factors was estimated following the *BYPASS* algorithm [27], implemented as the *SQUEEZE* option in *PLATON* [28]. A new data set, free of solvent contribution, was then used in the final refinement. All non-hydrogen atoms were refined with anisotropic atomic displacement parameters. H atoms were finally included in their calculated positions and treated as riding on their parent atom with constrained thermal parameters. Crystal data and details of data collection and refinement for **1** are summarized in table 2, and additional crystallographic details are provided in the cif file (Supplementary data). ORTEP views were drawn using OLEX2 software [29]. CCDC 1943145 contains the supplementary crystallographic data for this paper. These data can be obtained free of charge from The Cambridge Crystallographic Data Centre *via* www.ccdc.cam.ac.uk/data_request/cif

Accepted manuscript

Table 2 Crystallographic data, details of data collection and structure refinement parameters for compound **1**.

Empirical Formula	C_{44} H_{26} Br_4 N_4
Formula mass, g mol^{-1}	930.33
Collection *T*, K	150(2)
Crystal size (mm)	0.33 x 0.16 x 0.15
Crystal color	Blue
crystal system	Monoclinic
space group	*C* 2/c
a (Å)	27.018(3)
b (Å)	6.1841(7)
c (Å)	26.339(4)
β (°)	115.487(4)
V ($Å^3$)	630.5(5)
Z	4
D_{calcd} (g cm^{-3})	1.556
F(000)	1832
abs coeff (mm^{-1})	4.088
θ range (°)	3.028 to 27.476
range h,k,l	-32/34, -8/8, -34/34
No. total refl.	23992
No. unique refl.	4528
Comp. θ_{max} (%)	99.9
Max/min transmission	0.542 /0.446
Data/Restraints/Parameters	4528 / 0 / 235
Final *R* [I>2σ(I)]	R_1 = 0.0358 wR_2 = 0.0726
R indices (all data)	R_1 = 0.0520 wR_2 = 0.0784
Goodness of fit / F^2	1.013
Largest diff. Peak/hole (e$Å^{-3}$)	1.578 d -1.389

Accepted manuscript

2.4 Hirshfeld Surface (HS) determination

The analyses of the surfaces were mapped using CrystalExplorer [30], starting from the crystallographic information file (CIF) of **1**. The normalized contact distance (d_{norm}), defined in terms of d_e, d_i and the vdW raddi of the atoms, was calculated using Eq. 1, where the distance from the HS to the nearest nucleus internal (d_i) or external (d_e), with respect to the surface involved, and vdW is the van der Waals raddi of atoms, according to the literature [31].

$$d_{\text{norm}} = \frac{d_{\text{i}} - r_{\text{i}}^{\text{vdW}}}{r_{\text{i}}^{\text{vdW}}} + \frac{d_{\text{e}} - r_{\text{e}}^{\text{vdW}}}{r_{\text{e}}^{\text{vdW}}} \qquad \textbf{Eq. 1}$$

The dimensional (3D) HS map is generated by d_{norm}, and appear as red spots over a surface of close-contact interactions, responsible of molecular packing in the crystal lattice. Also, 3D d_{norm} surfaces can be plotted in 2D fingerprint representations, to quantitatively summarize, the nature and type of all intermolecular interactions present in the crystal packing. HS for **1**, mapped over d_{norm} (range -0.1027 to 3.3089Å), are illustrated in figure 3 (section 3.5).

3. Results and Discussions

3.1. Synthesis

The known symmetrical 5,10,15,20-tetrakis(4-bromophenyl)Porphyrin (**1**) [20] was first synthesized according to a conventional heating method [32] upon mixing equimolar amounts of 1*H*-Pyrrole and 4-bromobenzaldehyde in dichloromethane for 3 h, followed by an oxidation step using an excess of *p*-chloranil under reflux for 1 h (Scheme 1). Upon work-up and chromatographic purification, **1** was isolated as a microcrystalline purple solid in a quite good yield of 55%. Interestingly, this yield can be increased to 78% under microwave irradiation [17,18] for 20 min (Scheme 1 and section 2.2.2), after changing *p*-chloranil for propionic acid (1 mL) in 10 mL of CH_2Cl_2 (entry 2 of Table 1). However, variation of the amount of propionic acid has a dramatic impact on the yield of **1**, that drops

Accepted manuscript

to 8% when an excess of the organic acid is used (entry 6). This is probably due to an increasing generation of side and oxidation products, rendering difficult the purification and isolation of the targeted macrocycle **1**.

3.2. ^{1}H NMR spectroscopy

It is relevant to note that in the vast majority of ^{1}H NMR spectra of *meso*-substituted porphyrins, the signals associated to the NH protons located in the center of the porphyrinic ring are highly shielded, while the *meso*- and β-protons are unshielded due to the effect of the diamagnetic anisotropy presented by the aromatic macrocycle [32]. This property facilitates the identification of protons associated with the central nitrogen atoms that appear at -2.85 ppm for compound **1**, while those of the β-protons of the aromatic system show up around 8.00 ppm. This molecular target being a symmetric tetraphenyl-porphyrin, the signals observed in the spectrum can be analyzed in a simple way. One singlet for the protons in the β-system and two doublets for the magnetically non-equivalent protons of the 4-bromophenyl rings (see experimental section).

3.3. Description of the X-ray crystal structure

Single crystals suitable for X-ray structure investigation were obtained for the symmetrical *meso*-porphyrin **1** by vapor diffusion techniques (see Experimental Section). The molecular structure of **1** is displayed in Figure 1 with selected bond distances and angles given in Table 3. The symmetrical *meso*-porphyrin **1** crystallizes in the centrosymmetric space group *C* 2/c with half *meso*-porphyrin molecule per asymmetric unit, expanded by symmetry operations -x, -y, -z (see fig. 1). The single-crystal X-ray diffraction study confirms the formation of the tetra-substituted porphyrin through the condensation between 1*H*-Pyrrole and 4-bromobenzaldehyde. The interatomic C-N (range: 1.372(3) - 1.375(4) Å) and C-Br (1.907(3) and 1.898(3) Å) distances (see Table 3) are similar to others porphyrin- and bromine-based molecules [17,33]. In addition, the C-C bond distance through the molecular backbone reveals a strong π-delocalization of the macrocycle in a network of sp^2 hybridized carbon atoms (Table 3). The connected four pyrrole fragment complete an almost planar core with N(1) and N(2) atoms defining the N_4 basal plane. In addition, the pyrrole (mean plane) units shows a torsion angle of 10.75(2)

Accepted manuscript

and 4.03(2)º, respectively, with respect to the N_4-core (mean plane). On the other hand, the torsion angles exhibited by the phenyl rings with respect to the same core-plane are 66.54(1) and 56.50(1)º, respectively.

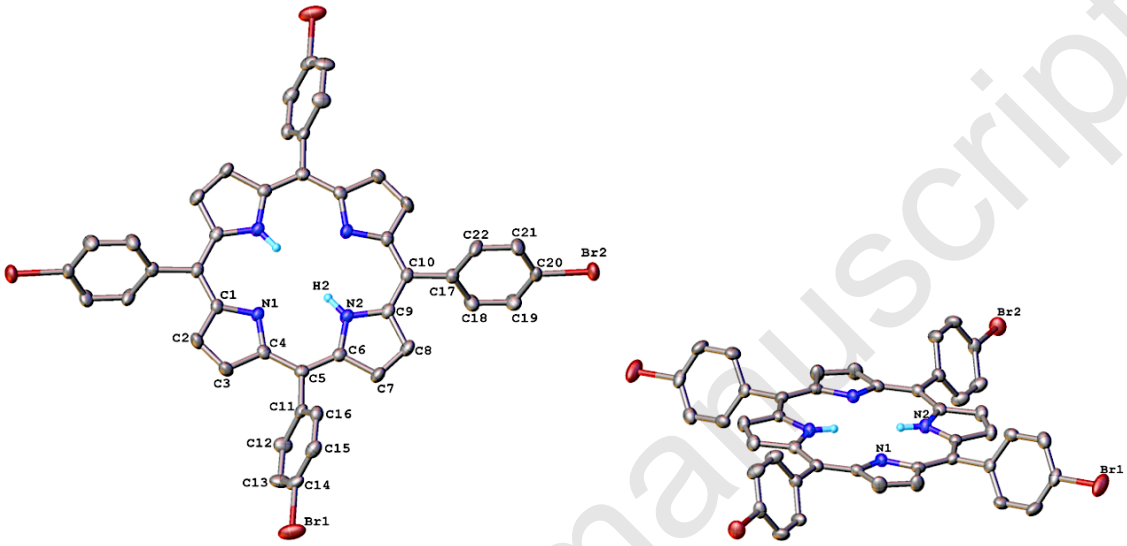

Fig. 1. Molecular structure of *meso*-porphyrin **1**, top view (*left*) and side view (*right*), with partial atom labelling scheme. Hydrogen atoms are omitted for clarity with exception of N-H fragments. Thermal ellipsoids are drawn at 70% probability and half unit of **1** was generated by symmetry operations -x, -y, -z.

Table 3 Selected bond distances (Å) and angles (°) for compound **1**.

Bond distances			
N(1)-C(1)	1.372(3)	N(2)-C(6)	1.374(4)
N(1)-C(4)	1.372(4)	N(2)-C(9)	1.375(4)
C(1)-C(10)$^{\#1}$	1.407(4)	C(6)-C(5)	1.399(4)
C(1)-C(2)	1.446(4)	C(6)-C(7)	1.434(4)
C(2)-C(3)	1.351(4)	C(7)-C(8)	1.358(4)
C(3)-C(4)	1.444(4)	C(8)-C(9)	1.433(4)
C(4)-C(5)	1.404(4)	C(9)-C(10)	1.401(4)
C(5)-C(11)	1.497(4)	C(10)-C(17)	1.496(4)
C(14)-Br(1)	1.907(3)	C(20)-Br(2)	1.898(3)
Bond angles			
C(1)-N(1)-C(4)	106.60(2)	C(6)-N(2)-C(9)	108.60(2)
N(1)-C(1)-C(10)$^{\#1}$	109.60(2)	N(2)-C(6)-C(5)	126.10(3)
N(1)-C(4)-C(5)	126.40(3)	N(2)-C(9)-C(10)	125.40(3)
C(4)-C(5)-C(6)	125.80(3)	C(9)-C(10)-C(1)$^{\#1}$	125.40(2)
C(1)-C(2)-C(3)	107.10(3)	C(6)-C(7)-C(8)	107.40(3)
C(2)-C(3)-C(4)	107.40(3)	C(7)-C(8)-C(9)	108.10(3)

Symmetry transformations used to generate equivalent atoms: #1 -x, -y, -z

Accepted manuscript

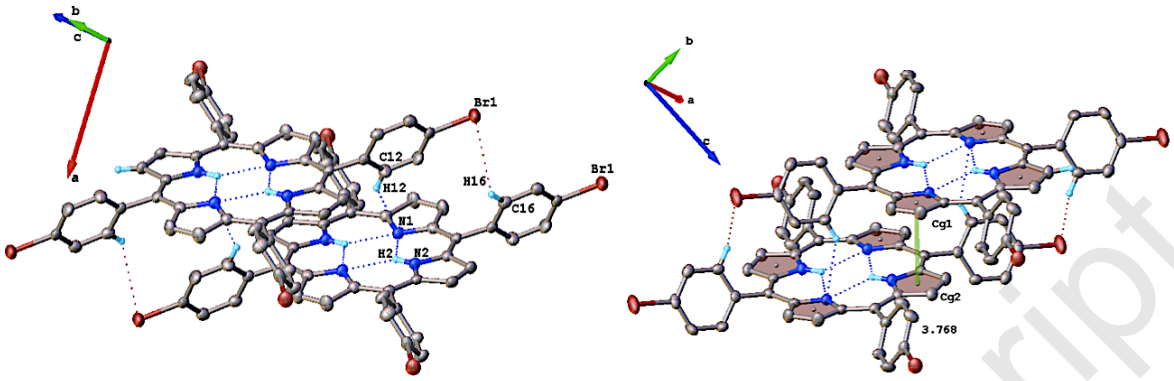

Fig. 2. *(left)* Inter- and intra-molecular H-bonds and (*right*) π-π close contact interactions determined from the crystal packing of **1**, showing a partial atom numbering scheme. Non relevant hydrogen atoms are omitted for clarity. Thermal ellipsoids are drawn at 60% probability.

3.4. Solid-state supramolecular interactions

The molecules of **1** are connected through a series of intermolecular hydrogen bonds (table 4 and figure 2). The projection of the packing shows an extended parallel-displaced disposition, possibly attributable to the π-stacking interactions between the aromatic systems and the bromine atoms (table 4, and figure 2(right)) due to an intermolecular close contact involving the two pyrrolic rings (Cg_1 and Cg_2), and between phenyl ring (Cg_3) and one bromine atom of each molecule. In addition, this arrangement can be explained by the hydrogen bonds formed beside parallel-displaced molecular-chains (figure 2 (left)).

Table 4 Close contact interactions in crystal lattice of **1**.

Hydrogen bond calculated by X-ray diffraction				
Donor-H ··· Acceptor	*D-H(Å)*	*H ··· A(Å)*	*D ··· A(Å)*	*D-H ··· A(°)*
N(2)-H(2)··· N(1)[a]	0.880(3)	2.360(2)	2.910(3)	120.8(2)
C(12)-H(12)··· N(1)[b]	0.950(3)	2.599(2)	3.384(4)	140.21(19)
C(16)-H(16)··· Br(1)[b]	0.950(3)	3.170(5)	3.742(3)	120.5(2)
π-π stacking interactions determined by X-ray diffraction				
Centroid-Centroid	*Distance(Å)*	*Twist angle(°)*		

Accepted manuscript

Cg_1-Cg_2[b]	3.768(16)	85.6(14)
Cg_3-Br(2)[b]	3.336(8)	3.00(2)

[a] intramolecular H-bond; [b] neighboring molecule; where: Cg_1 = C6-(N2)-C9; Cg_2 = C1-(N1)-C4; Cg_3 = C11-C16.

3.5. Hirshfeld Surface Analysis (HSA)

The supramolecular interactions observed by X-ray diffraction are, surely, determined by indirect approximations. In this regard, performing HSA is a good way to complement the presence of several intermolecular contacts. This analysis is defined as the electron density boundary surfaces between the molecules in a crystal lattice [31].

During the mapping, the surfaces are kept transparent for the visualization of various supramolecular interactions responsible for the packing stabilization. The HS of **1** mapped in Fig. 3 shows the most important supramolecular interaction centered in the -CH and -Br fragments (red spots), which highlights the close contact through which the intermolecular interaction in the crystal lattice takes place. The color intensity can be used for visualizing the strength of the interactions. In this regard, the most important interaction is that exhibited by C-H···Br bond between two molecules, over the weaker interactions C-H···N previously described in Table 4.

Accordingly, the analysis of the HS plots obtained for **1**, shows two important red spots (see figure 3), corresponding to C-H···Br interactions, and are more important than the present C-H···N interactions previously described in table 4 (light-red spots). On the other hand, the analysis of the expansion pack considering the most important interactions (red spots), reveals the important role of these close contact interactions in **1** (fig. 4). This important supramolecular interaction provides high thermal and moisture stability to the crystal packing, and allows us to project this type of complexes for diverse applications in solid phase. The crucial role of these close contact interactions can be contrasted by the analysis of the fingerprint plots (fig. 5). The most relevant C-H···Br interactions, present in the crystal packing, represent the 32.5% over the total HS (fig. 5, left and middle). In this context, the 2D fingerprint plots are useful in the quantification of different interactions. The plots of **1** (fig. 5) shows the H···Br interactions with a shortest *de* + *di* distance ~3.00

Accepted manuscript

Å, and the 23.3% (including the reciprocal contacts) of the total HS. In addition, the most abundant close contact interaction at long distance is H···H with a 40.1% of the total HS. Finally, the presence of π···π stacking interactions are evidenced by *de* + *di* ≈ 3.50Å (4.6% C···C + 2.7% C···N) (figure 2). Considering this analysis, the most important supramolecular interactions, responsible of the stability of the crystal lattice, are the CH···Br and CH···N close contacts.

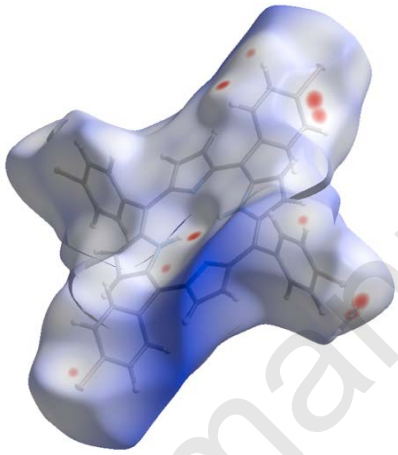

Fig. 3. Views of the d_{norm} Hirshfeld surface plotted for **1**. Intermolecular H-bonds are described in Table 4 and text.

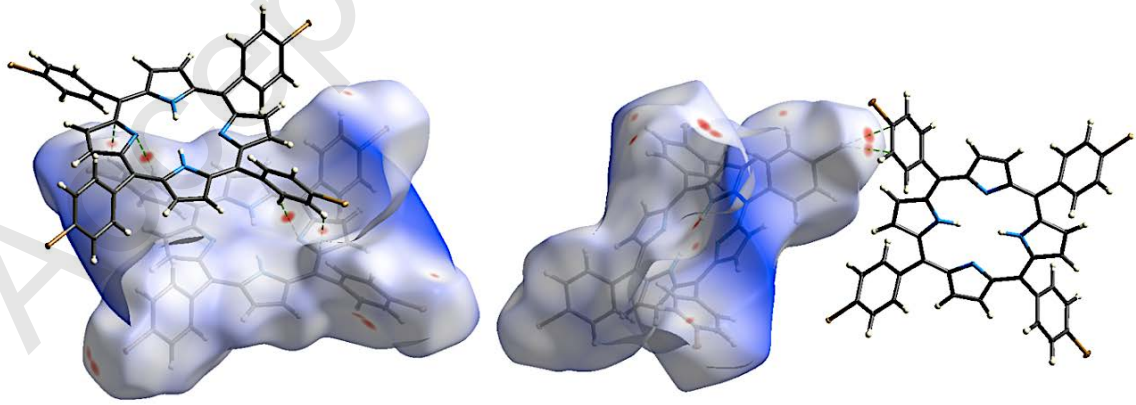

Accepted manuscript

Fig. 4. Relevant hydrogen bond (left) and close contact Br···C interactions (right) determined by HS plotted over d_{norm} for the crystal packing of **1**. Thermal ellipsoids are drawn at 20% probability.

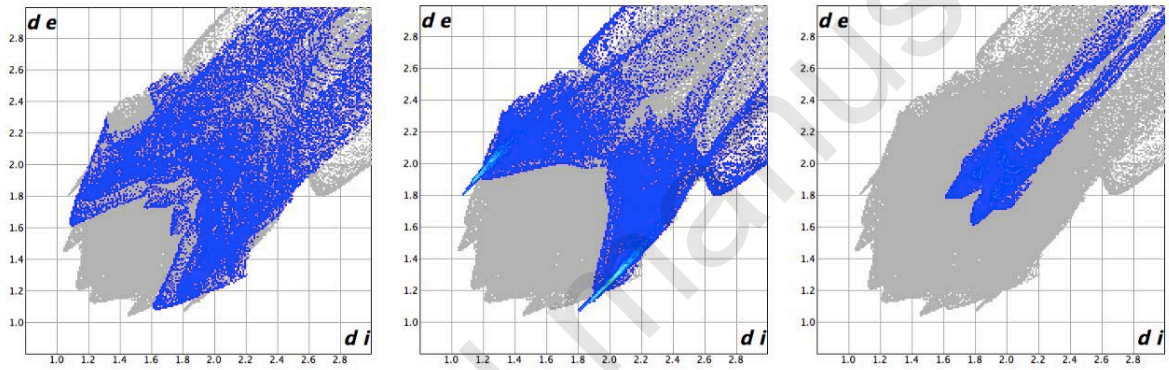

Fig. 5. Decomposed fingerprint plots related with HS areas and contributions (including reciprocal contacts) to the total HS for close contact interactions of C···H(left), Br···H (middle), and C···Br(right) present in the crystal packing of **1**.

4. Conclusions

In this paper, the 5,10,15,20-*tetrakis*(4-bromophenyl)Porphyrin (**1**) *is* successfully prepared by conventional and microwave assisted techniques, characterized and monitored by means of various physical methods. The microwave assisted preparation gives quite high yields in the preparation of this precursor, decreasing the presence of side-products in the synthesis, and reducing the reaction time and volume of organic solvent used. Also, the crystal structure of this macrocyclic compound has been studied. It is shown that the solid-state structures are influenced by the intermolecular interactions. The presence of several

Accepted manuscript

intermolecular contacts, including hydrogen bonds and π···π stacking close contact interactions were visually gained by Hirshfeld Surface analysis. 2D fingerprint plots provided an estimation of the influence of such interactions on the crystal lattice and stability. The synthetic versatility and simplicity of the microwave assisted approach, allowing a facile scale-up of the procedure, depicted here suggest application in the chemical design of selective molecular scaffolds for multi-centered binding and reactivity in coordination and organometallic chemistry.

Acknowledgements

Financial support from the Fondo Nacional de Desarrollo Científico y Tecnológico [FONDECYT (Chile), grant No. 11160658 (IR: N.N.)] and the Vicerrectoría de Investigación y Desarrollo, Universidad de Concepción (Chile), grant VRID Iniciación No. 216.021.034-10-1.0IN (IR: N.N.), the CNRS and the Université de Rennes 1 is gratefully acknowledged. This research has been performed as part of the Chilean-French International Associated Laboratory for "Multifunctional Molecules and Materials" (LIA M3-CNRS N°1207). F.V-G. thanks also the CONICYT (Chile) for support of a National Master Scholarship (UdeC). E. M-C. thanks also the FONDECYT (Chile), grant No. 11160658 for support of a undergraduate scholarship (UdeC).

Appendix A. Supplementary data

Supplementary data to this article can be found online at https://doi.org/10.1016/j.molstruc.2019.xx.xxx.

References

[1] For an overview of photo-, electro- and bio-chemical properties of porphyrins and applications, see The Chemical and Physical Behavior of Porphyrin Compounds and Related Structures, ed. A.D. Adler, Ann. N.Y. Acad. Sci., vol. 206, (1973) 5-761.

[2] T. Tanaka, A. Osuka, Conjugated porphyrin arrays: synthesis, properties and applications for functional materials, Chem. Soc. Rev. 44 (2015) 943–969.

[3] M. Jurow, A.E. Schuckman, J.D. Batteas, C.M. Drain, Porphyrins as molecular electronic components of functional devices, Coord. Chem. Rev. 254 (2010) 2297–2310.

[4] M.O. Senge, M. Fazekas, E.G.A. Notaras, W.J. Blau, M. Zawadzka, O.B. Locos,

Accepted manuscript

E.M. Ni Mhuircheartaigh, Nonlinear Optical Properties of Porphyrins, Adv. Mater. 19 (2007) 2737–2774.
[5] S.J. Lee, J.T. Hupp, Porphyrin-containing molecular squares: Design and applications, Coord. Chem. Rev. 250 (2006) 1710–1723.
[6] L.-L. Li, E.W.-G. Diau, Porphyrin-sensitized solar cells, Chem. Soc. Rev. 42 (2013) 291–304.
[7] M. Urbani, M. Grätzel, M.K. Nazeeruddin, T. Torres, Meso-Substituted Porphyrins for Dye-Sensitized Solar Cells, Chem. Rev. 114 (2014) 12330–12396.
[8] S. Erbas-Cakmak, D.-A. Leigh, C.-T. McTernan, A.-L. Nussbaumer, Artificial Molecular Machines, Chem. Rev. 115 (2015) 10081–10206.
[9] D. Feng, Z.-Y. Gu, J.-R. Li, H.-L. Jiang, Z. WenWei, H.-C. Zhou, Zirconium-Metalloporphyrin PCN-222: Mesoporous Metal-Organic Frameworks with Ultrahigh Stability as Biomimetic Catalysts, Angew. Chem. Int. Ed. 51 (2012) 10307-10310.
[10] J.S. Lindsey, Synthetic Routes to meso-Patterned Porphyrins, Acc. Chem. Res. 43 (2010) 300–311.
[11] A.D. Adler, F.R. Longo, J.D. Finarelli, J. Goldmacher, J. Assour, L. Korsakoff, A Simplified Synthesis for *meso*-tetraphenylporphin, J. Org. Chem. 32 (1967) 476.
[12] N. Asano, S. Uemura, T. Kinugawa, H. Akasaka, T. Mizutani, Synthesis of Biladienone and Bilatrienone by Coupled Oxidation of Tetraarylporphyrins, J. Org. Chem. 72 (2007) 5320-5326.
[13] R.A.W. Johnstone, M.L.P.G. Nunes, M.M. Pereira, A.M.D. Rocha Gonsalves, A.C. Serra, Improved Syntheses of 5,10,15,20-Tetrakisaryl- and Tetrakisalkylporphyrins, Heterocycles 43 (1996) 1423-1438, and references cited therein.
[14] H. Shy, P. Mackin, A.S. Orvieto, D. Gharbharan, G.R. Peterson, N. Bampos, T.D. Hamilton, The two-step mechanochemical synthesis of porphyrins, Faraday Discuss. 170 (2014) 59-69.
[15] C.M. Drain, X. Gong, Synthesis of *meso* substituted porphyrins in air without solvents or catalysts, Chem. Commun. (1997) 2117-2118.
[16] A. Petit, A. Loupy, P. Maiuard, M. Momenteau, Microwave Irradiation in Dry Media: A New and Easy Method for Synthesis of Tetrapyrrolic Compounds, Synth. Commun. 22 (1992) 1137-1142.
[17] B.F.O Nascimento, M. Pineiro, A.M.d'A. Rocha Gonsalves, M. Ramos Silva, A. Matos Beja, J.A. Paixão, Microwave-Assisted Synthesis of Porphyrins and Metalloporphyrins: a Rapid and Efficient Synthetic Method, J. Porphyr. Phthalocyanines. 11 (2007) 77–84.
[18] S.M.S. Chauhan, B.B. Sahoo, K.A. Srinivas, Microwave-assisted synthesis of 5,10,15,20-Tetraaryl porphyrins, Synth. Commun. 31 (2001) 33-37.
[19] H.-G. Jin, X. Jiang, I.A. Kühne, S. Clair, V. Monnier, C. Chendo, G. Novitchi, A.K. Powell, K.M. Kadish, T. Silviu Balaban, Microwave-Mediated Synthesis of Bulky Lanthanide Porphyrin-Phthalocyanine Triple-Deckers: Electrochemical and Magnetic Properties, Inorg. Chem. 56 (2017) 4864-4873.
[20] J.B. Kim, J.J. Leonard, F.R. Longo, Mechanistic study of the synthesis and spectral properties of *meso*-tetraarylporphyrins, J. Am. Chem. Soc. 94 (1972) 3986–3992.
[21] O.B. Locos, D.P. Arnold, The Heck reaction for porphyrin functionalisation: synthesis of meso-alkenyl monoporphyrins and palladium-catalysed formation of unprecedented meso–β ethene-linked diporphyrins, Org. Biomol. Chem. 04 (2006) 902–916.

Accepted manuscript

[22] S. Hiroto, Y. Miyake, H. Shinokubo, Synthesis and Functionalization of Porphyrins through Organometallic Methodologies, Chem. Rev. 117 (2017) 2910–3043.
[23] W.L.F. Armarego, C.L.L. Chai, Purification of Laboratory Chemicals, Butterworth-Heinemann-Elsevier, Sixth edn., 2009.
[24] S. Drouet, A. Merhi, D. Yao, M.P. Cifuentes, M.G. Humphrey, M. Wielgus, J. Olesiak-Banska, K. Matczyszyn, M. Samoc, F. Paul, C.O. Paul-Roth, Cubic nonlinear optical properties of new zinc tetraphenyl porphyrins peripherally functionalized with electron-rich Ru(II) alkynyl substituents, Tetrahedron. 68 (2012) 10351–10359.
[25] G.M. Sheldrick, SHELXT - Integrated space-group and crystal-structure determination, Acta Crystallogr. Sect. A 71 (2015) 3–8.
[26] G.M. Sheldrick, Crystal structure refinement with SHELXL, Acta Crystallogr. Sect. C 71 (2015) 3–8.
[27] P. Van Der Sluis, A.L. Spek, BYPASS: an effective method for the refinement of crystal structures containing disordered solvent regions, Acta Crystallogr. Sect. A 46 (1990) 194–201.
[28] A.L. Spek, research papers Single-crystal structure validation with the program PLATON research papers, J. Appl. Crystallogr. 36 (2003) 7–13.
[29] O.V Dolomanov, L.J. Bourhis, R.J. Gildea, J.A.K. Howard, H. Puschmann, OLEX2: a complete structure solution, refinement and analysis program, J. Appl. Crystallogr. 42 (2009) 339–341.
[30] M.J. Turner, J.J. McKinnon, S.K. Wolff, D.J. Grimwood, P.R. Spackman, D. Jayatilaka, M.A. Spackman, CrystalExplorer17, (2017). http://hirshfeldsurface.net.
[31] M.A. Spackman, D. Jayatilaka, Hirshfeld surface analysis, CrystEngComm. 11 (2009) 19–32.
[32] The Porphyrin Handbook: Vol. 18 Multiporphyrins, Multiphthalocyanines and Arrays, Edited by: K. M. Kadish, K.M. Smith, R. Guilard, Elsevier Science, 2012.
[33] T.A. Dar, R. Tomar, R.M. Mian, M. Sankar, M.R. Maurya, Vanadyl β-tetrabromoporphyrin: synthesis, crystal structure and its use as an efficient and selective catalyst for olefin epoxidation in aqueous medium, RSC Adv. 9 (2019) 10405–10413.

Accepted manuscript